

## The QUAX Experiment

D. Alesini, D. Babusci, A. D’Elia (AR), D. Di Bari(Tecn.), D. Di Gioacchino, C. Gatti (Resp.), S. Lauciani (Tecn.), C. Ligi, G. Maccarrone, D. Moricciani, G. Papalino(Tecn.), G. Pileggi (Tecn.), A. Rettaroli (Dott.), S. Tocci (AR)

### 1 Introduction

In 2021 the CSN2 approved the QUAX proposal for an experiment for galactic-axion search with a standard Sikivie type haloscopes in the 8-11 GHz frequency range. The QUAX experiment will operate two complementary apparata, one located in the Laboratori Nazionali di Legnaro and the other in the Laboratori Nazionali di Frascati. The two haloscopes will be working at two different frequency ranges, implementing two different types of microwave cavity and quantum limited detectors. The decision came after three years of QUAX R&D during which the haloscope at LNL reached in 2021 the sensitivity to QCD axions. In a couple of years, with a realistic scan bandwidth of O(1) GHz feasible for both set-ups, we will be able to probe the yet unexplored region between 8.5 to 11 GHz, corresponding to the axion mass range from 34  $\mu\text{eV}$  to 44  $\mu\text{eV}$ . The physics reach is plotted in figure 1.

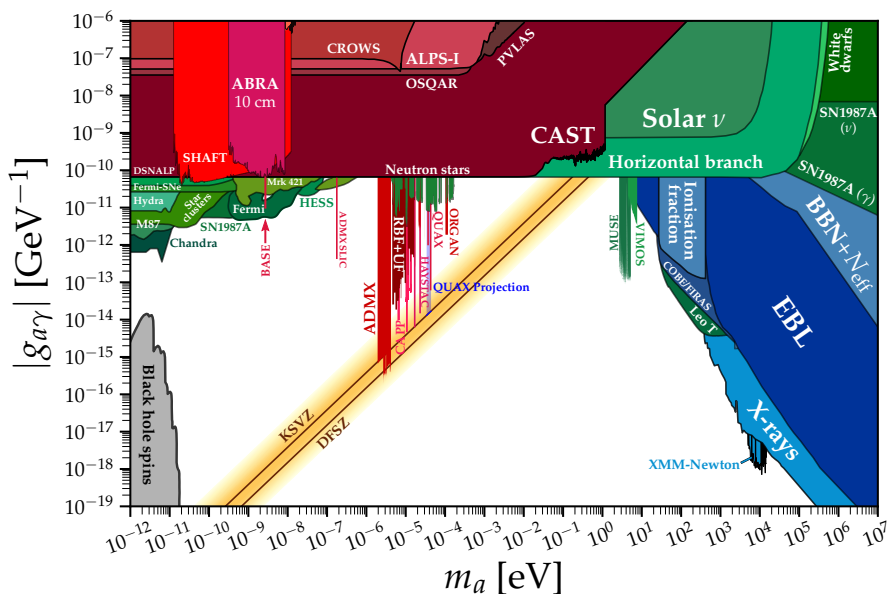


Figure 1: Projections for the sensitivity of QUAX with the two haloscopes compared to existing limits <sup>1)</sup>.

In section 2 we present the axion search by QUAX published in 2021 showing sensitivity

Table 1: Noise contributions estimated at the cavity resonance frequency. “Vacuum” is the contribution of quantum fluctuations of vacuum. The room temperature HEMT (A2) contribution is negligible. “Cables” refers to RF attenuation of cables, with the only effect of reducing the overall gain.

Source	Gain [dB]	Noise Temp. [K]	Input Noise [K]
Cavity	–	0.078	0.078
Vacuum	–	0.25	0.25
JPA	18	0.25	0.25
Cables	-3	–	–
HEMT (A1)	30	8	0.25
Total			0.83

to QCD axions in the 40  $\mu\text{eV}$  mass range. In section 3 we present the published result on the measurement of the quality factor of a dielectric cavity able to operate in a strong magnetic field with a quality factor of about 700,000. Finally in section 4 we discuss the ongoing installation of the LNF haloscope.

## 2 Search for Invisible Axion Dark Matter of mass $m_a = 43 \mu\text{eV}$ with the QUAX- $a\gamma$ Experiment

An haloscope of the QUAX- $a\gamma$  experiment composed of an OFHC-Cu cavity inside an 8.1 T magnet and cooled to  $\sim 200$  mK was put in operation for the search of galactic axion with mass  $m_a \simeq 43 \mu\text{eV}$ . The power emitted by the resonant cavity was amplified with a Josephson Parametric Amplifier whose noise fluctuations are at the Standard Quantum Limit (SQL). With the data collected in about 1 h at the cavity frequency  $\nu_c = 10.40176$  GHz the experiment reached the sensitivity necessary for the detection of galactic QCD-axion setting the 90% confidence level (CL) limit to the axion-photon coupling  $g_{a\gamma\gamma} < 0.766 \cdot 10^{-13} \text{ GeV}^{-1}$  <sup>2)</sup>.

The haloscope, assembled at Laboratori Nazionali di Legnaro (LNL), is composed by a cylindrical OFHC-Cu cavity, with inner radius of 11.05 mm and length 210 mm, inserted inside the 150 mm diameter bore of an 8.1 T superconducting (SC) magnet of length 500 mm. The total volume of the cavity is  $V = 80.56 \text{ cm}^3$ . The whole system is hosted in a dilution refrigerator with base temperature of 90 mK. Each cavity endplate hosts a dipole antenna in the holes drilled on the cavity axis. The cavity was treated with electrochemical polishing to minimize surface losses. We measured the resonant peak of the  $TM_{010}$  mode at 150 mK and magnet on with a Vector Network Analyzer obtaining the frequency  $\nu_c = 10.4018$  GHz and an unloaded quality-factor  $Q_0 = 76,000$  in agreement with expectations from simulation performed with the ANSYS HFSS suite. During data-taking runs, the cavity was critically coupled to the output radiofrequency (RF) line and the loaded quality-factor was measured to be about  $Q_L = 36,000$ .

The RF setup is shown in Fig. 2. The main improvement in this setup is the preamplification stage obtained with the JPA described in <sup>3)</sup>. It has noise temperature expected at the quantum-limit of about 0.5 K (including 0.25 K from vacuum fluctuations) and a resonance frequency tunable between 10 and 10.5 GHz by varying the pump amplitude and frequency and by applying a small magnetic field for fine regulation. After tuning the resonance frequency of the JPA to that of the cavity we measured a gain of 18 dB in a 10 MHz bandwidth. The estimated contributions to the total noise are summarized in table 1.

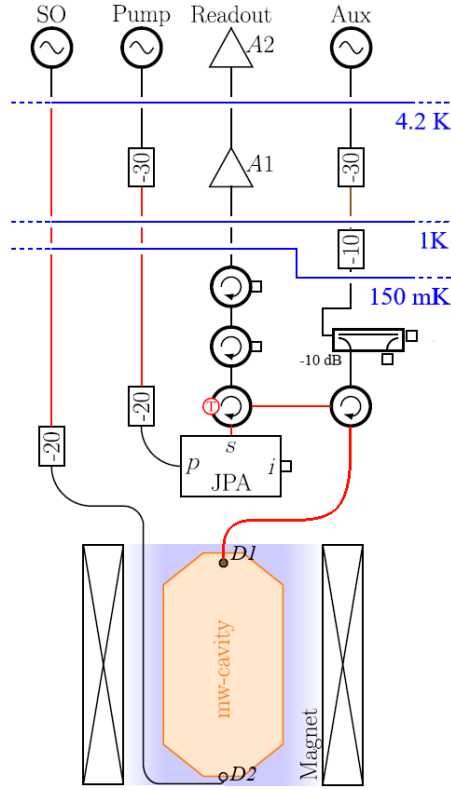


Figure 2: Schematics of the experimental apparatus. The microwave cavity (orange) is immersed in the uniform magnetic field (blue shaded region) generated by the magnet (crossed boxes). A1 and A2 are the cryogenic and room-temperature amplifiers, respectively. The JPA amplifier has three ports: signal (s), idler (i), and pump (p). Superconducting cables (red) are used as transmission lines for RF signals from 4 K stage to 150 mK stage. Thermometers (red circled T) are in thermal contact with the resonant cavity and the signal port on the JPA. Attenuators are shown with their reduction factor in decibels. The horizontal lines (blue) identify the boundaries of the cryogenic stages of the apparatus, with the cavity enclosed within the 150 mK radiation shield. The magnet is immersed in liquid helium.

We performed the axion search for a total time  $\Delta t = 4203$  s looking for power in excess in the Power Spectrum distribution. In order to extract the residuals, we modeled the system composed of the cavity and the readout line with an equivalent electrical circuit based on transmission-line formalism. Since no relevant excess was observed we set an upper limit on the axion-photon coupling constant. This is shown in Fig. 3 as a function of the tested axion masses, shown with a colored filled area, together with a solid purple line showing the expected limit in case of no signal. The reference upper limit of our search is the value at the maximum sensitivity (the minimum of purple line of Fig. 3),  $g_{a\gamma\gamma}^{\text{CL}} < 0.766 \cdot 10^{-13} \text{ GeV}^{-1}$  at 90% C.L.

In Fig. 4 we compare the limit  $g_{a\gamma\gamma}^{\text{CL}}$  that we observed, in a mass window  $\Delta m_a = 3.7$  neV centered at the mass  $m_a = 43.0182 \mu\text{eV}$ , with those obtained in previous searches.

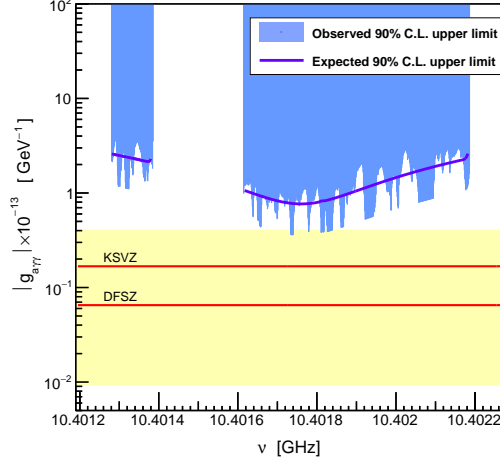


Figure 3: 90% single-sided C.L. upper limit for the axion coupling constant  $g_{a\gamma\gamma}$ . Each point corresponds to a test axion mass in the analysis window. The solid curve represents the expected limit in case of no signal. The yellow region indicates the QCD axions model band. We assume  $\rho_a \sim 0.45 \text{ GeV}/\text{cm}^3$ .

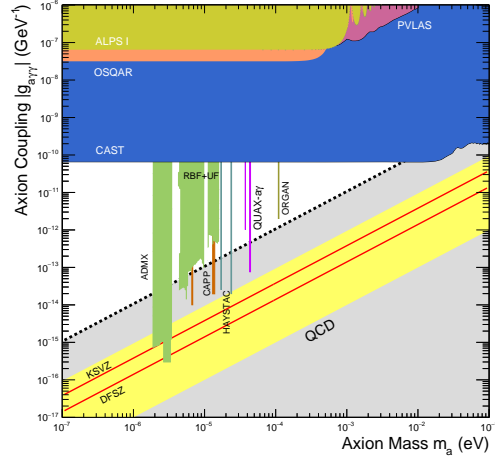


Figure 4: Aggregate plot of the limits on  $g_{a\gamma\gamma}$  obtained from the main axion search experiments; the two limits obtained by the QUAX collaboration are highlighted in purple. The grey area identifies the region where axions could be found, with the yellow band and the two solid red lines identifying the coupling predicted by the KSVZ and DFSZ models and its uncertainty.

### 3 Realization of a high quality factor resonator with hollow dielectric cylinders for axion searches

We realized and characterized a high quality-factor resonator composed of two hollow-dielectric cylinders with its pseudo-TM<sub>030</sub> mode resonating at 10.9 GHz frequency (Fig. 5). The quality

factor was measured at the temperatures 300 K and 4 K obtaining  $Q_{300\text{K}} = (150,000 \pm 2,000)$  and  $Q_{4\text{K}} = (720,000 \pm 10,000)$  respectively, the latter corresponding to a gain of one order of magnitude with respect to a traditional copper cylindrical-cavity with the corresponding  $\text{TM}_{010}$  mode resonating at the same frequency. Contrary to Type-I superconducting cavities, dielectric cavities can operate in presence of strong, multi tesla, magnetic fields with large implications for axion dark-matter searches. Numerical simulations show that frequency tuning of several hundreds MHz is feasible <sup>4</sup>).

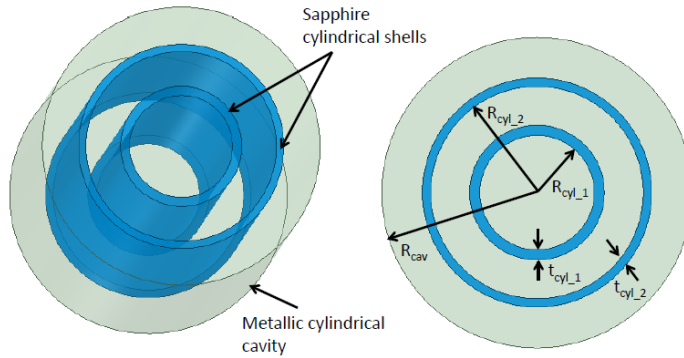


Figure 5: Sketch of the cavity with dielectric cylindrical shells.

In the proposed configuration, with two shells, the selected mode is the pseudo- $\text{TM}_{030}$ , as given in Fig. 6, where we show the electric field amplitude in one quarter of the cavity. The cavity resonant-frequency  $f_{res}$  was tuned to 10.9 GHz and the dielectric shells geometrical parameters ( $R_{cyl_1}$ ,  $R_{cyl_2}$ ,  $t_{cyl_1}$ ,  $t_{cyl_2}$  as defined in Fig. 5) were optimized to minimize the losses in the outer walls. The choice of this frequency was mainly given by the possibility of incorporating the resonator inside the detection chain developed within the QUAX haloscope.

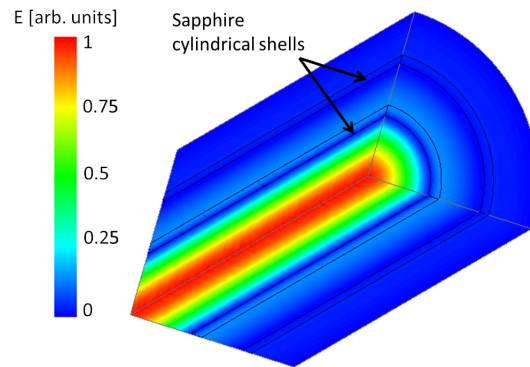


Figure 6: (colour online) Electric field amplitude of the pseudo  $\text{TM}_{030}$  mode.

Two fine-grid sapphire-tubes 200 mm long were purchased from ROSTOX-N. Their optical axes (C-axis, 0001) are oriented along the cylinder axis of symmetry within one degree, as stated by the manufacturer. We measured, with 4 points per side, the tubes diameters with a coordinate-

measuring device at Laboratori Nazionali di Frascati. The tubes were then sent to Laboratori Nazionali di Legnaro (LNL) for assembly inside the copper cavity. Three photographs of partial assemblies of the dielectric cavity are shown in Fig. 7. The final assembly of the sapphire shells is done with only one end-cap removed and the cavity in the vertical position.

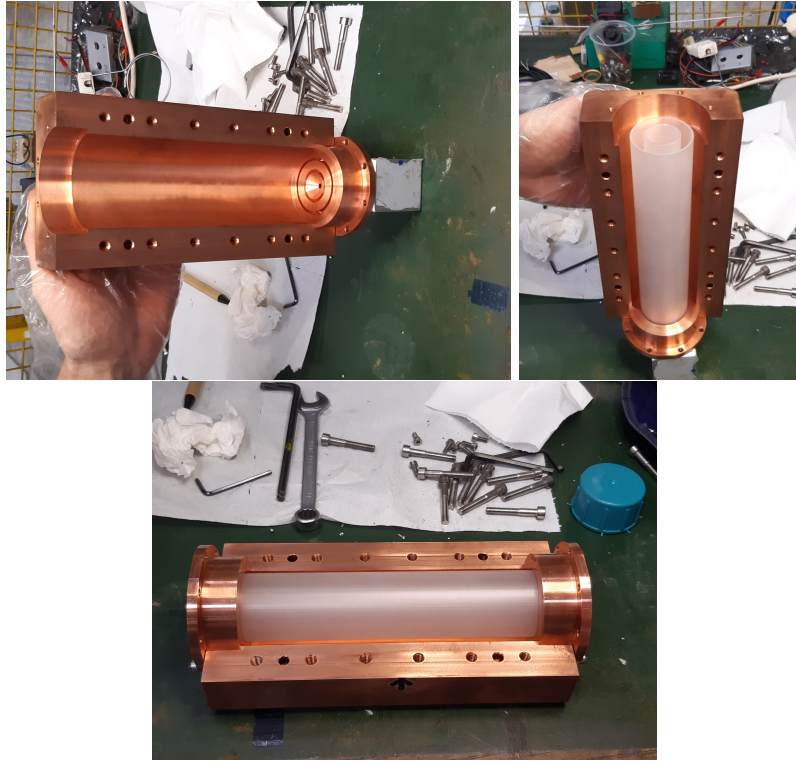


Figure 7: Partial assemblies of the dielectric cavity.

We characterized the resonant modes of the dielectric cavity at LNL in a LHe-cryostat at 5.4 K. We connected the cavity to two fixed antennas subcritically coupled to the pseudo- $\text{TM}_{030}$  mode and placed it inside a vacuum chamber designed to allow operation inside cryogenic dewars. The vacuum chamber is equipped with two rf feedthroughs and a thermometer measuring the temperature of the cavity. The thermometer was mounted on the external surface of the resonant cavity, thermally coupled to it. The temperature scale was calibrated within 1 K. The spectrum of the resonant modes was measured at 300 and 5.4 K with a Vector Network Analyzer (VNA). Transmission and reflection parameters taken at 5.4 K are shown in Fig. 8 as measured from the port with higher coupling to the cavity, while on the other port the reflected signal was barely visible. The measured loaded quality factor is  $Q_L = 632,000$ . The unloaded quality factor is calculated as  $Q_{030} = (1 + k) \times Q_L$  where  $k \sim (1 - S_{11}(\nu_{030})) / (1 + S_{11}(\nu_{030}))$  is the coupling to the antenna. We obtain  $Q_{030} = (720,000 \pm 10,000)$  a very large quality factor if compared with copper cavities at these frequencies and temperatures with typical quality factor of less than 100,000. The error reflects the stability of the measurement in time and the uncertainty on the determination of the coupling  $k$ . We also observed a 10% variation by moving the whole cryostat in order to change the alignment of the sapphire tubes. However, missing a mechanical-movement system in our setup, we could not investigate this effect further and we postpone it until the movement

system will be available.

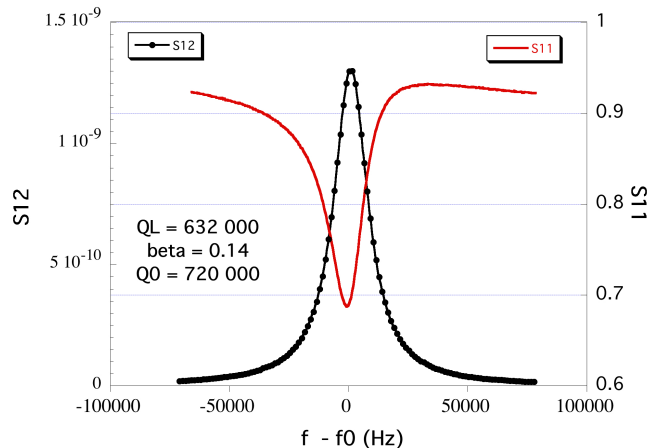


Figure 8: Transmission and reflection parameters as a function of frequency for the pseudo- $\text{TM}_{030}$  mode at 10.916 GHz at 5.4 K.

#### 4 The LNF Haloscope

The second QUAX haloscope is under construction at the COLD laboratory at LNF. A dilution refrigerator was put in operation, a Leiden CF-CS110-1000, with a Sumitomo pulse-tube with 1.5 W cooling power at 4.2 K, a base temperature of 8 mK and a mixing chamber plate of 490 mm diameter. The cooling power of the dilution refrigerator was measured to be  $450 \mu\text{W}$  at 100 mK recently extended up to  $700 \mu\text{W}$  by improving the pumping capacity with a new turbo pump. The refrigerator is instrumented with four 0.86 mm BeCu-Ag-CuNi coaxial-lines thermalized at different temperatures down to 4 K down to the mixing chamber plate. The signal is read out through a fifth dedicated superconducting coaxial line connecting a sample holder at 10 mK, designed to host an amplifier or a single photon-device, to the HEMT amplifier mounted on the 4 K plate and, with a normal line, up to an SMA feedthrough on a 300 K flange and room temperature electronics.

The LNF haloscope will operate with a multicavity scheme with the cavities tuned to different frequencies as shown in fig. 9. Up to 7 resonant cavities with frequency between 8.5 and 10 GHz may fit inside a 9 T magnet (fig. 10) with 10 cm bore taking into account the thickness of cryostat radiation-shields and cavity walls. A successful operation of the cavities at the same frequency would further improve the scanning rate of the experiment. A realistic scan bandwidth of  $O(1)$  GHz is feasible covering the yet unexplored region from about 9 to 10 GHz, while the haloscope at LNL would cover the region from 10 to 11 GHz, corresponding in total to the axion mass range from about  $35 \mu\text{eV}$  to  $45 \mu\text{eV}$ .

The magnet, manufactured by American Magnetics Inc., has a height of 486 mm and cold bore diameter of 100 mm. The maximum current in the coils is of about 90 A for a 9 T field at the center of the magnet, reducing to about 7 T at a distance of 10 cm along the axis. Above the cold bore volume, a second superconducting set of coils is present, oppositely oriented with respect to the main coils, to reduce the field to less than 50 Gauss, thus providing a region where superconducting devices, requiring zero magnetic fields, can be housed.

The signals from multiple cavities must be combined with minimum loss before the pre-amplification stage. To this end we designed a planar diplexer to combine the signals from two

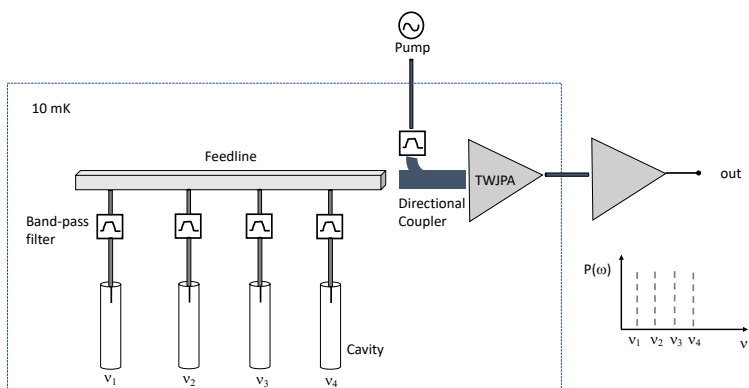


Figure 9: Sketch of the multicavity scheme of the QUAX-LNF haloscope

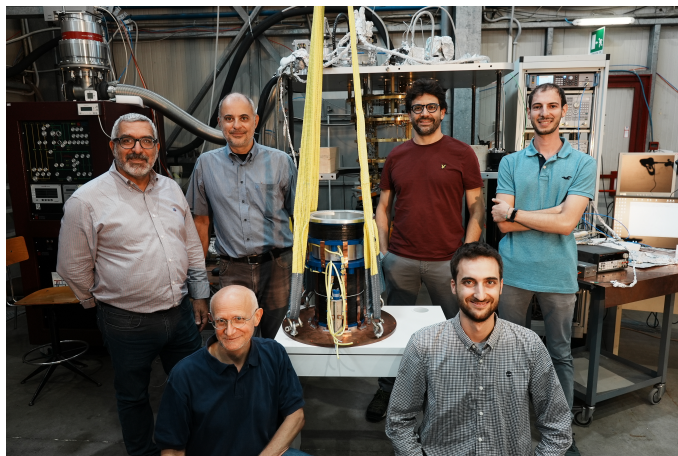


Figure 10: The arrival of the 9T magnet at COLD lab.

cavities with different resonant frequencies (left panel of fig. 11). Adding more cavities will require coupling more diplexers or designing a multiplexer with more ports. The minimum frequency separation between the cavities is set by the ability to tune it. We performed simulations with a tuning rod inserted in a cylindrical cavity resonating at 8.5 GHz. The result is shown on the right panel of figure 11. The frequency of the mode of interest, the TM<sub>010</sub>, changes by about 200 MHz from 8.6 to 8.8 GHz by rotating the tuning rod of about 90 degrees. With four resonant cavities separated in frequency by 200 MHz we could span about 1 GHz of axion frequency range at the same time.

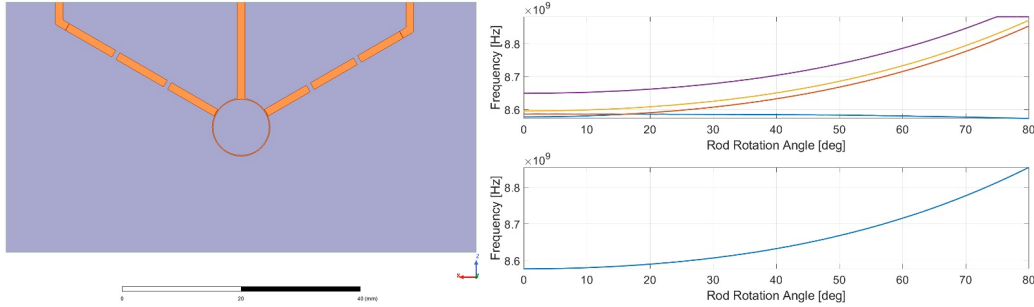


Figure 11: Left: Design of the diplexer which combines signals at 5.5 and 6 GHz coming from the two lateral input-ports to the output-port in the middle. The two microstrip filters at the entrance of the input-ports avoid unwanted interference between the two signals. Simulation shows low loss ( $\ll 1$  dB) and few hundred MHz bandwidth. Right: Variation of the modes frequencies as a function of the angle of the tuning rod inside the resonant cavity.

The Low-noise amplification of signals from the array of resonant cavities requires a large bandwidth quantum-limited amplifier. To this end we plan to use Traveling Wave Josephson Parametric Amplifiers (TWJPA) wide band quantum amplifiers made of a coplanar waveguide composed of an array of RF-SQUIDS. We are presently testing such amplifiers within the DART WARS INFN project. The device has expected amplification ranging from 25 to 35 dB in a bandwidth from 5 to 10 GHz.

Resonant cavities will be fabricated using Type II superconductors allowing to improve the quality factor with respect to copper cavities even when operating in a magnetic field of several Tesla<sup>5</sup>). We already measured a quality factor above 300,000 inside a 6 T magnetic field with a NbTi cavity, and YBCO cavity was characterized at 7 GHz at IBS-CAPP showing a quality factor of about 330,000 in a 8 T magnetic field. Further tests are ongoing at LNF with Nb<sub>3</sub>Sn within the DOE-SQMS and INFN-SAMARA projects.

In 2022, we plan a pilot run with a single tunable resonant-cavity made of copper. The microwave cavity, a cylindrical OFHC copper cavity, with height 246 mm and inner radius 13.51 mm, corresponding to a total volume of 0.141 liters, was fabricated at LNF workshop and electropolished at LNL (left panel of fig. 12). The body is divided into two semi-cylinders that will be sealed with screws; in this way, additional endcaps that would interrupt the flow of the rf currents causing losses are not necessary. At the top and bottom of the cavity, the holes for the input and readout antennas are put at the center of the endcaps. We measured the cavity transmission spectrum at room temperature with a VNA. The spectrum, shown in the right panel of fig. 12 shows the first resonant peak coupled to the antenna, corresponding to the TM<sub>010</sub> mode, at about 8.5 GHz.

In conclusion, the optimization of the magnetic volume together with the quantum-limited readout and superconductive cavities will allow the LNF haloscope to perform an axion search with

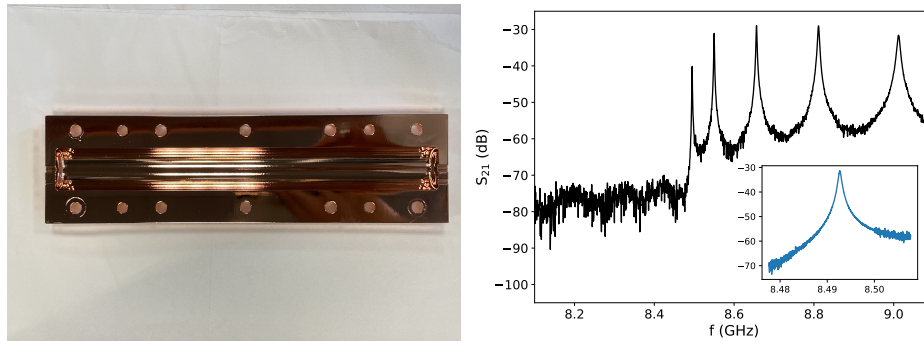


Figure 12: Left) Half of the electropolished OFHC copper cavity that will be used for measurements with the rst tuning system. Right) 1 GHz-wide cavity spectrum. The inset shows the zoom on the TM010 mode at 8.5 GHz.

a scan speed up to about 20 MHz per day. Further improvements are expected by the development of single microwave photons detectors under study with the project INFN-SIMP or the H2020-FET project Supergalax.

## 5 List of Conference Talks by LNF Authors in Year 2021

1. A. Rettaroli, “Probing the axion-photon interaction with QUAX experiment: status and perspectives,” 16th Patras Workshop on Axions, WIMPs and WISPs (Online).
2. C. Gatti, “Search for Axion Dark Matter with the QUAX Haloscopes,” EPS HEP 2021 (online).
3. C. Gatti, “Search for Axion Dark Matter with the QUAX Haloscopes,” International Workshop Searching for Galactic Axions and Superconducting Devices with Quantum Efficiency October 2021 at IBS-CAPP (online).
4. F. Sirghi and C. Gatti, “L’attività di ricerca del Laboratorio di Frascati dell’INFN,” 107o Congresso Nazionale della Società Italiana di Fisica SIF2021.
5. C. Gatti, “Boosting Axions Searches With Quantum Sensing,” IEEE 14th Workshop on Low Temperature Electronics WOLTE14 (Online).

## 6 Publications

- D. Alesini et al., “Realization of a high quality factor resonator with hollow dielectric cylinders for axion searches,” Nuclear Inst. and Methods in Physics Research, A 985 (2021) 164641.
- D. Alesini et al., “Search for invisible axion dark matter of mass  $m_a = 43 \mu\text{eV}$  with the QUAX- $a\gamma$  experiment,” PHYSICAL REVIEW D 103, 102004 (2021).
- C. Gatti, P. Gianotti, C. Ligi, M. Raggi, P. Valente, “Dark Matter Searches at LNF,” Universe 2021, 7, 236. <https://doi.org/10.3390/universe7070236>
- A. Alimenti et al., “Impact of Superconductors’ Properties on the Measurement Sensitivity of Resonant-Based Axion Detectors,” Instruments 2022, 6, 1. <https://doi.org/10.3390/instruments6010001>

- C. Gatti, “Boosting Axion Searches with Quantum Sensing,” 2021 IEEE 14th Workshop on Low Temperature Electronics (WOLTE), 2021, pp. 1-4, doi: 10.1109/WOLTE49037.2021.9555436.

### Acknowledgement

Partially supported by EU through FET Open SUPERGALAX project, grant agreement N.863313

### References

1. Plot generated with code from <https://cajohare.github.io/AxionLimits/> by Ciaran Ohare.
2. D. Alesini et al., “Search for invisible axion dark matter of mass  $m_a = 43 \mu\text{eV}$  with the QUAX- $\alpha\gamma$  experiment,” *PHYSICAL REVIEW D* 103, 102004 (2021).
3. N. Roch et al., “Widely tunable, nondegenerate three-wave mixing microwave device operating near the quantum limit,” *Phys. Rev. Lett.* 108, 147701 (2012).
4. D. Alesini et al., “Realization of a high quality factor resonator with hollow dielectric cylinders for axion searches,” *Nuclear Inst. and Methods in Physics Research, A* 985 (2021) 164641.
5. A. Alimenti et al., “Impact of Superconductors’ Properties on the Measurement Sensitivity of Resonant-Based Axion Detectors,” *Instruments* 2022, 6, 1. <https://doi.org/10.3390/instruments6010001>